Leaf and canopy photosynthesis of a chlorophyll deficient soybean mutant

Karolina Sakowska[1,2,3], Giorgio Alberti[4,5], Lorenzo Genesio[5,6*], Alessandro Peressotti[4], Gemini Delle Vedove[4], Damiano Gianelle[3,6], Roberto Colombo[7], Mirco Rodeghiero[3], Cinzia Panigada[7], Radosław Juszczak[2], Marco Celesti[7], Micol Rossini[7], Matthew Haworth[8], Benjamin W. Campbell[9], Jean-Philippe Mevy[10], Loris Vescovo[3], M. Pilar Cendrero-Mateo[11], Uwe Rascher[11], and Franco Miglietta [5,6,12]

[1]Institute of Ecology, University of Innsbruck, Sternwartestrasse 15, 6020 Innsbruck, Austria

[2]Meteorology Department, Poznan University of Life Sciences, Piatkowska Street 94, 60-649 Poznan, Poland

[3]Sustainable Agro-Ecosystems and Bioresources Department, Research and Innovation Centre, Fondazione Edmund Mach, Via E. Mach 1, 38010 S. Michele all'Adige (TN), Italy

[4]Department of Agricultural, Food, Environmental and Animal Sciences, University of Udine, via delle Scienze, 206, 33100 Udine, Italy

[5]Institute of Biometeorology, National Research Council (CNR- IBIMET), Via Caproni 8, 50145 Florence, Italy

[6]Foxlab Joint CNR-FEM Initiative, Via E. Mach 1, 38010 San Michele all'Adige, Trento, Italy

[7]Department of Earth and Environmental Sciences, University of Milano-Bicocca, Piazza della Scienza 1, 20126 Milan, Italy

[8]Tree and Timber Institute, National Research Council (CNR - IVALSA), Florence, Italy

[9]University of Minnesota, St. Paul, MN, USA

[10]Institut Méditerranéen de Biodiversité et d'Ecologie Marine et Continentale (IMBE), Aix Marseille Université, Université Avigon, CNRS 7263/IRD 237, 3 place Victor Hugo, 13331 Marseille Cedex 03, France

[11]Institute of Bio- and Geosciences, IBG-2: Plant Sciences, Forschungszentrum Jülich GmbH, Leo-Brandt-Str., 52425 Jülich, Germany

[12]IMèRA, Institut D'Etudes Avancés de l'Universitè Aix-Marseille, 2 Place Le Verrier, Marseille, France

*** Corresponding author:**

Lorenzo Genesio

Tel.: +39 055 3033711

E-mail: l.genesio@ibimet.cnr.it

Present address: CNR- IBIMET, Via Caproni 8, 50145 Florence, Italy

Keyword index: steady state and dynamic photosynthesis, NPQ relaxation

Abstract

The photosynthetic, optical and morphological characteristics of a chlorophyll-deficient (Chl-deficient) “yellow” soybean mutant (MinnGold) were examined in comparison with two green varieties (MN0095 and Eiko).

Despite the large difference in Chl content, similar leaf photosynthesis rates were maintained in the Chl-deficient mutant by offsetting the reduced absorption of red photons by a small increase in photochemical efficiency and lower non-photochemical quenching (NPQ). When grown in the field, at full canopy cover, the mutants reflected a significantly larger proportion of incoming shortwave radiation, but the total canopy light absorption was only slightly reduced, most likely due to a deeper penetration of light into the canopy space. As a consequence, canopy-scale gross primary production and ecosystem respiration were comparable between the Chl-deficient mutant and the green variety. However, total biomass production was lower in the mutant, which indicates that processes other than steady state photosynthesis, caused a reduction in biomass accumulation over time. Analysis of NPQ relaxation and gas exchange in Chl-deficient and green leaves after transitions from high to low light conditions suggested that dynamic photosynthesis might be responsible for the reduced biomass production in the Chl-deficient mutant under field conditions.

Introduction

Chlorophyll-deficient mutants are common in plants (Highkin, 1950; Gengenbach *et al*., 1970; Specht *et al*., 1975; Li *et al*. 2013). Mutations leading to 100% albino plants are fatal, while other types of mutations that simply reduce chlorophyll (Chl) content (Daloso *et al*. 2014) lead to plants that can successfully complete their lifecycle. These plants have frequently been used to investigate how carbon uptake in leaves scales with Chl-content (Benedict *et al*., 1972). Similar or higher leaf photosynthetic capacities (Li *et al*., 2013; Slattery *et al*., 2017; Kirst *et al*., 2017; Gu *et al*., 2017a; Gu *et al*., 2017b*)* have been observed in Chl-deficient varieties when compared to "green" counterparts of the same species. The most common interpretation of such an effect is that reduced Chl-content facilitates a more even distribution of light within the mesophyll (Vogelmann *et al*., 1996; Vogelmann & Evans, 2002), which attenuates photoprotection (non-photochemical quenching - NPQ) and thus leads to an increase in the photochemical efficiency of photosystem II (Φ_{PSII}) (Li *et al*., 2013). As a consequence, more carbon dioxide (CO_2) can be fixed per absorbed photon and per unit of leaf area, and the same photosynthetic rates can be maintained despite increased light reflectance/transmission (Ort & Melis, 2011).

The idea that canopies of Chl-deficient plants can attain photosynthetic rates higher than those of the more common "green" cultivars has already been postulated (Drewry *et al*., 2014) and modelled (Song *et al*., 2017). When Chl-deficient crops are grown in the field and reach full canopy cover, they are not only expected to distribute light more uniformly across the leaf, but also throughout the entire canopy. Due to a higher light transmittance of the upper canopy layers, plants with lower Chl-content should allow more photons to reach the lower layers of the canopy, which results in a more uniform illumination of the canopy and a smaller fraction of the canopy being subject to light

saturation (Long *et al*. 2006; Walker *et al*., 2017; Gu *et al*., 2017a).

The use of Chl-deficient crops is also expected to have an effect on the land surface energy balance. Reduced Chl-content may lead to an increase in reflectance and transmittance, particularly in the region of the spectrum outside the Chl absorption peaks. This may increase the overall surface shortwave albedo, which is currently considered to be an effective bio-geophysical strategy in the mitigation of increasing atmospheric radiative forcing (Bright *et al*., 2016). An increase in albedo may also potentially lead to significant water savings, unless water vapor canopy conductance is modified (Drewry *et al*. 2014; Zamft & Conrado 2015). Recent model experiments have shown that the reduction of shortwave radiative forcing of croplands by increasing their albedo can mitigate the magnitude of future heatwaves (Davin *et al*., 2014), as well as offset a portion of the expected global greenhouse gases-driven rise in near-surface air temperatures (Ridgwell *et al*., 2009; Hirsch *et al*., 2017).

The main objective of this study is to elucidate the functional relationship between chlorophyll content and gross and net primary production (GPP and NPP, respectively) by integrating leaf and canopy measurements. For this purpose, a comprehensive set of measurements using soybean Chl-deficient mutant and two green varieties were performed at both the leaf and canopy scale on plants grown in pots and in the field.

Materials and Methods

Plant material and growth conditions

This study compared the MinnGold soybean Chl-deficient mutant with two green soybean varieties: MN0095 (University of Minnesota, USA) and Eiko (Asgrow, USA). The mutant

phenotype is the result of a nonsynonymous substitution in a magnesium chelatase ChlI subunit leading to plants with a "yellow" or "golden" phenotype with approximately 80% less chlorophyll than the green varieties (Campbell *et al*., 2014).

In 2015, plants were grown in pots and in the field at the experimental farm of the University of Udine, in Italy. Both experiments were designed to explore photosynthetic and optical properties of MinnGold and MN0095. Seeds were sown in one thousand 3.5 l pots filled with agricultural soil, spatially arranged in a fully randomized design with five replicates. The simultaneous field trial consisted of three replicates per line, planted in 7.0 x 7.0 m plots at a density of 35 plants m^{-2}. These experiments revealed that MinnGold and MN0095 were not in the same maturity group. Therefore, when a larger field experiment aiming also at biomass production and yield assessment was designed in 2016, MN0095 was replaced with Eiko - a commercial cultivar of the same maturity group as MinnGold (I-). Within this experiment, MinnGold and Eiko were sown in two non-replicated 1 ha plots at the experimental farm of the University of Udine at a density of 40 plants m^{-2}.

In 2017, plants of all the three accessions (MinnGold, Eiko and MN0095) were grown in pots to comparatively assess any differences in photosynthetic performance.

The entire set of measurements performed over a period of 3 years is summarized in Table S1.

Leaf scale measurements

Leaf gas exchange and pulse-amplitude modulated (PAM) fluorescence

The measurements in 2015 were made approximately 65 days after emergence on the most recently fully expanded leaves of pot- and field-grown MinnGold and MN0095 plants using automated gas

exchange systems (Li-6400, LI-COR Inc., Lincoln, NE, USA) equipped with blue/red LED light sources (6 cm^2 Li-6400-02B chamber and 2 cm^2 Li-6400-40 Leaf Chamber Fluorometer). Photosynthetic capacity was assessed by measuring net assimilation (A; μmol m^{-2} s^{-1}) versus the inter-cellular CO_2 concentration (C_i; μmol mol^{-1}) at saturating photosynthetic photon flux density (PPFD: 1500 μmol m^{-2} s^{-1}) by adjusting the CO_2 concentration in the cuvette in a series of steps: 400, 300, 200, 100, 50, 400, 600, 800, 1200, 1600, 2000 μmol mol^{-1}. Light-response curves (A/PPFD) were determined by measuring A at different PPFD levels (1500, 1100, 700, 300, 100 and 0 μmol m^{-2} s^{-1}) and a CO_2 concentration of 400 μmol mol^{-1} in the cuvette. A/PPFD curves for pot-grown plants were also obtained with an additional light source (metal halide lamp, Powerstar HQI-T 2000 W/N 230 V, OSRAM, Munich, Germany) with different spectral characteristics to the LEDs within the Li-6400 cuvette.

Mesophyll conductance to CO_2 (g_m; mol m^{-2} s^{-1}) in both field and pot-grown leaves was determined from the A/C_i curves using the approach of Ethier & Livingston (2004). Photorespiration (R_{PR}; μmol m^{-2} s^{-1}) was quantified to verify possible changes in the carboxylation efficiency between the two accessions. R_{PR} was estimated from measurements of A under saturating light intensity and a cuvette CO_2 concentration of 400 μmol mol^{-1} at both 21% and 2% O_2 concentrations (Keys *et al.*, 1977).

The NPQ measurements using PAM technique were made on field-grown plants and were preceded by covering four randomly chosen plants of the two accessions with non-transparent ventilated boxes and leaving them to dark-adapt overnight. Minimal (F_o) and maximal (F_m) fluorescence were measured on four dark-adapted leaves using the Li-6400-40 chamber. Maximal fluorescence of light-adapted leaves (F_m') was then determined after at least 25 min exposure to high intensity light (2000 μmol m^{-2} s^{-1}). NPQ (Maxwell & Johnson, 2000) was determined as:

$$NPQ = \frac{Fm - Fm'}{Fm'} \quad (1)$$

Light-adapted PAM fluorescence parameters (F_m' and F_s - steady state fluorescence) were also measured using the same Li-6400-40 chamber on a larger number of both potted (n=11 for each accession) and field (n=30 for each accession) leaves from the upper canopy during determination of light-saturated assimilation. The ΦPSII (Genty *et al*., 1989) was then estimated as:

$$\phi PSII = \frac{Fm' - Fs}{Fm'} \quad (2)$$

The above measurements were complemented by comparing light response curves measured in 2017 on pot-grown plants of MinnGold, MN0095 and Eiko. This was undertaken to verify that leaf scale photosynthetic rates in the two "green" accessions were comparable. These additional measurements were performed on the second trifoliate leaves, 30 days after emergence.

Leaf optical properties

Reflectance and transmittance of the most recently fully expanded leaves were measured in 2015 and 2016 on field-grown plants of MinnGold, MN0095 and Eiko under solar irradiance by means of a FieldSpec Handheld spectrometer (ASD, Colorado, USA), coupled with a FluoWat leaf clip (Van Wittenberghe *et al*., 2013). Leaf reflectance and transmittance were used to derive light absorbance in different spectral regions and further calculate the fraction of PPFD absorbed by Chl-deficient and green leaves (fAPPFD$_{LEAF}$)

Leaf area, leaf mass, pigments and nitrogen concentration measurements

Leaf area was determined using a LI-3000C Portable Leaf Area Meter (LI-COR Inc., Lincoln, NE,

USA), and the fresh weight of individual leaves was measured. Circular discs (1 cm diameter) were cut from each leaf, weighed and used for determination of chlorophyll a and b and carotenoids by UV-VIS spectroscopy (Lichtenthaler, 1987; extraction with methanol and acetone in 2015 and 2016, respectively). The remaining part of the leaves were dried at 80°C for 48 hours and used to determine the nitrogen (N) content using a Vario MICRO Cube Elemental Analyzer (Elementar Analysensysteme GmbH, Langenselbold, Germany). Specific leaf mass was obtained by measuring leaf area and dry weight on another set of randomly selected fully expanded leaves.

Non-photochemical quenching relaxation

NPQ relaxation in fluctuating light conditions was assessed as the decay of non-photochemical quenching and in particular of zeaxanthin-dependent quenching (qZ) in the dark, after imposing a number of high/low light cycles to the leaves of MinnGold and Eiko that were grown in pots in the spring and fall of 2017. Measurements were performed using a Fluorescence Monitoring System (FMS2-Hansatech, King's Lynn, UK), and the variations in illumination were created using an artificial light. In the adopted protocol, soon after the determination of F_m on four dark-adapted leaves, two minutes of illumination with 2000 μmol m^{-2} s^{-1} followed by two minutes with 200 μmol m^{-2} s^{-1} of light were imposed in six cycles. Measurements of variable-light adapted F_m' were performed over 10 minutes in the dark at variable frequencies. NPQ was calculated for each F_m' measurement and then normalized to the maximum, and a double exponential model (Kromdijk *et al*., 2016) was fitted to the dark relaxation NPQ data. The procedure was applied to both unifoliate and trifoliate leaves of the two accessions.

The translation of faster/slower NPQ relaxation into different leaf CO_2 uptake rates was examined

on four leaves of pot-grown MinnGold and Eiko plants. As for the NPQ relaxation, the leaves were exposed to six cycles of 2000/200 μmol m^{-2} s^{-1} of light and the dynamics of CO_2 uptake were measured using the Li-6400 gas exchange system at 2 seconds intervals for 10 minutes after a sharp transition from high to low light.

Canopy scale measurements

Canopy scale gas exchange

Diurnal patterns of canopy scale CO_2 exchange were measured from July 21st to 27th 2016 at full canopy cover by means of a closed dynamic portable chamber system, in which air is circulated at a constant flow rate (0.7 l min^{-1}) between the chamber headspace and a portable CO_2 analyzer (LI-840, LI-COR Inc., Lincoln, NE, USA). Measurements were made in four subplots of the MinnGold and Eiko fields. The system consisted of a transparent (3 mm thick Plexiglas® - Evonik Industries, Darmstadt, Germany) and non-transparent chamber (3 mm thick white PVC) used to measure net ecosystem exchange (NEE) and ecosystem respiration (R_{eco}), respectively (Juszczak *et al*., 2012; Acosta *et al*., 2017). During the measurements, the chambers were placed on square PVC collars (0.75 x 0.75 m) inserted into the soil 26 days prior to the start of the measurements. Due to differences in the canopy height, chambers with a total volume (including the PVC collar) of 0.47 and 0.61 m^3 were used on MinnGold and Eiko, respectively. To ensure representative sampling of the air, the air inside the chamber was mixed by a set of computer fans (1.4 W, 1500 rpm each) fixed to the north-facing wall of the chamber at a minimum height of 40 cm above the ground and oriented toward the vegetation canopy. Fan speed was set to generate sufficient turbulence to provide adequate mixing in the chamber headspace and a realistic canopy wind speed profile in

respect to height (<1 m s^{-1} at the top of the canopy). The air temperature increment inside the chamber headspace was minimized using a passive cooling system described in Acosta *et al*. 2017, which also prevented condensation of water vapor on the chamber walls during the measurements. Air temperature inside each chamber was measured using a radiation-shielded thermistor (T-107, Campbell Scientific, USA). Maximum chamber closure time was 1.5 minutes during NEE measurements and 2.5 minutes during R_{eco} measurements. The maximum temperature increase inside the chamber during a single measurement was less than 1.5 °C, while the maximum PPFD change did not exceed 10% after the canopy closure. Fluxes were calculated on the basis of the rate of change in the chamber CO_2 concentration during the closure time, as described by Hoffmann *et al*. (2015). The gross primary production (GPP) was calculated as the difference between consecutively measured NEE and R_{eco} (in total 78 and 75 coupled NEE and R_{eco} measurements for MinnGold and Eiko, respectively). Heterotrophic respiration (R_h) was measured on additional collars (in total 42 and 39 measurements for MinnGold and Eiko, respectively), in which the vegetation was completely removed one month before the measurements to eliminate the autotrophic component of soil respiration. Autotrophic respiration (R_a) was then estimated by subtracting R_h from R_{eco}. Soil temperature at a depth of 2 and 5 cm (T-107, Campbell Scientific, USA), air temperature at a height of 30 cm (T-107 with radiation shield, Campbell Scientific, USA) and incident PPFD (SKP215, Skye Instruments Ltd, UK) were measured at 5 second intervals.

Fraction of photosynthetic photon flux density absorbed by the canopy

The fraction of PPFD absorbed by the canopy ($fAPPFD_{CANOPY}$; -) was quantified in summer 2016 by measuring all the terms of the photosynthetic radiation balance, *i.e*. the downward PPFD incident

at the top the canopy, the downward PPFD transmitted through the canopy (T_c; μmol m^{-2} s^{-1}), the upward PPFD reflected from soil and canopy (R_{cs}; μmol m^{-2} s^{-1})and the upward PPFD reflected from soil (R_s; μmol m^{-2} s^{-1}). The fAPPFD$_{CANOPY}$ was calculated using the following equation, where APPFD$_{CANOPY}$ (μmol m^{-2} s^{-1}) is the absorbed PPFD:

$$f\mathrm{APPFD}_{\mathrm{CANOPY}} = \frac{\mathrm{PPFD}-\mathrm{T_C}-\mathrm{R_{CS}}+\mathrm{R_S}}{\mathrm{PPFD}} = \frac{\mathrm{APPFD}_{CANOPY}}{\mathrm{PPFD}} \quad (3)$$

The measurements were performed with a SunScan probe (Delta-T Devices Ltd., Cambridge, UK) under clear sky conditions (July 22nd to 23rd, 2016) in six randomly chosen plots located within the MinnGold and Eiko fields. A set of four measurements (two with the sensor centered on the rows, and two with the sensor placed between the rows) were taken with the probe oriented parallel to the rows (North-South orientation). Before and after each measurement, the values of the incident PPFD were recorded to evaluate the stability of the incident radiation and then averaged. R_s measurements were performed in an adjacent bare soil field. The APPFD$_{CANOPY}$ at the time of the canopy scale CO_2 exchange measurements was calculated by multiplying the mean fAPPFD$_{CANOPY}$ of the Chl-deficient or green canopies by the incident PPFD measured at the local meteorological station.

Surface energy balance and transpiration

In 2016, the two soybean experimental fields (MinnGold and Eiko) were equipped with two four band net radiometers (CNR-1, Kipp & Zonen, Delft, the Netherlands) to monitor (at 1 Hz scan frequency) the surface energy balance (Rn - net radiation) between incoming shortwave and

longwave radiation versus surface-reflected shortwave and outgoing longwave radiation of fully developed canopies. Data were averaged over 1 minute.

Canopy transpiration was measured by means of heat-balance sap-flow gauges (Peressotti & Ham, 1996), where heat is applied to the entire circumference of the stem encircled by a heating tape and the sap flow is obtained by measuring the difference in the fluxes of heat into and out of the heated section of the stem (Sakuratani, 1981). Ten gauges were installed on an equivalent number of plants of each accession and the fluxes were calculated at half-hour intervals from July 22nd to August 8th to obtain reliable estimates of the amount of water transpired.

Leaf area index and biomass production

The biomass produced by MinnGold and Eiko canopies (NPP) was quantified after the canopy CO_2 exchange measurements in 2016 (July 27th) by harvesting all of the plants (R5 growth stage) within each chamber collar. Leaves, stems, pods, and roots of each plant were separated manually and then dried at 65°C for 48 hours to determine the biomass allocation to individual organs. Leaf area per collar (LA; m^2) was measured using a LI-3000C Portable Leaf Area Meter (LI-COR Inc., Lincoln, NE, USA) and leaf area index (LAI; m^2 m^{-2}) was calculated by dividing LA by the collar surface area.

Statistical analysis

All data in the text, tables and figures are reported as mean ± standard error (s.e.), unless otherwise indicated. Depending on the type of analysis, accessions were compared using one or two-way ANOVA followed by Tukey's test. The nonparametric Mann-Whitney-Wilcoxon U-test was

instead used when ANOVA assumptions (*i.e*. normal distribution and homogenous variance of data) were violated. All statistical analysis were performed in STATA 10.1 (© StataCorp, College Station, TX, USA).

Results

Leaf level

At steady state conditions (i.e. after complete adaptation to the conditions inside the Li-6400 cuvette), MinnGold and MN0095 leaves showed almost identical light response curves (A/PPFD). Further measurements confirmed the same light response for Eiko (Figure S1). When light absorption was taken into account ($APPFD_{LEAF}$), MinnGold showed slightly higher, although not significant, assimilation rate per absorbed photon ($A/APPFD_{LEAF}$) (Figure 1; Figure S1). Photosynthetic response to intercellular CO_2 concentration at saturating light (A/C_i; Figure 1; Table S2), as well as R_{PR} (Table S2) were not altered by chlorophyll deficiency. At saturating light intensity (1500 μmol m^{-2} s^{-1}) and ambient CO_2 concentration (400 μmol mol^{-1}), MinnGold fixed a mean of 0.28 μmol CO_2 s^{-1} per mg of Chl, while this value was only 0.05 in the MN0095. The instantaneous Nitrogen Use Efficiency (NUE_i), defined as the ratio between A and N-content per unit leaf area, was larger in the mutant than in the green accession (10.9 vs. 7.7 μmol CO_2 s^{-1} g N^{-1}, respectively).

The reduced Chl-content of the leaves (Table 1) resulted in a reduction in the $fAPPFD_{LEAF}$ (Figure 2) and an increase in transmittance and reflectance (Figure S2) measured under solar irradiance. More detailed analysis of the $fAPPFD_{LEAF}$ in different spectral regions indicated that this reduction was negligible in the proximity of the blue peak (-1.8% at 458-462 nm), larger in the red peak (-4.5% at 670-674 nm), and very significant in the green region (-42% at 550-554 nm).

Φ_{PSII} was closely related to A in both accessions (Figure 3). The 8.7% higher Φ_{PSII} in the Chl-deficient mutant would suggest that a greater proportion of the absorbed light was used in photochemistry. Moreover, a significantly lower NPQ was observed in the Chl-deficient mutant than in MN0095

(1.66±0.25 vs 2.08±0.13, respectively; p-value=0.036), when measured using the PAM technique in the field.

However, NPQ relaxation after a sudden transition from high to low light was always slower in the mutant, with larger differences for the unifoliate than the trifoliate leaves (Figure 4A and Figure 4B, respectively; Table S3). CO_2 assimilation reflected the observed pattern in NPQ relaxation. When light dropped from 2000 to 200 μmol m^{-2} s^{-1}, net CO_2 assimilation declined significantly in both accessions. After fast relaxation due to energy-dependent quenching (qE), assimilation started to increase gradually during the zeaxanthin-dependent quenching (qZ) phase, but at different paces for MinnGold and Eiko. In the green leaves, faster NPQ relaxation led to a more rapid recovery of CO_2 fixation rate under low light. Due to the slower NPQ relaxation, the CO_2 assimilation of the Chl-deficient mutant did not reach steady state values within the entire measurement period (Figure 5).

Canopy level

When grown in the field the Chl-deficient canopies reflected a significantly higher fraction of the incoming shortwave radiation than the green canopy. At maximum canopy cover in the second half of July 2016, MinnGold reflected on average 14% more light than Eiko. Albedo was 0.26 and 0.29 for Eiko and MinnGold, respectively (Figure S3). Such a change in the surface energy balance translated into a significant decrease in canopy transpiration measured by sap-flow gauges (Figure 6A) and into a marginal decrease in surface canopy temperature derived from outgoing long-wave radiation (-0.38% on average; Figure 6B). Measurements of reflected and transmitted PPFD revealed a slight, but significant difference in $f\mathrm{APPFD}_{\mathrm{CANOPY}}$ of the two accessions (0.89±0.02 and

0.95±0.02 for MinnGold and Eiko, respectively, p-value<0.001). This difference was due to different reflectance components (R_{cs}/PPFD was equal to 9.68±0.59% in MinnGold and 2.98±0.12% in Eiko) and not transmittance, which was very similar. In both canopies, only a tiny fraction of the incident PPFD penetrated through the canopy and reached the soil surface (T_c/PPFD equal to 1.42±2.06% in MinnGold and 1.81±2.47% in Eiko).

When averaged over the entire measurement period, the response curves of GPP to absorbed light were similar for MinnGold and Eiko (Figure 7A). No statistical difference was observed in R_{eco} of the two varieties (Figure 7B; Table S4) and the contribution of R_a to R_{eco} was equal to 77% and 71% in MinnGold and in Eiko, respectively (Table S4).

No significant differences in plant density and LAI were detected between the two accessions (Table 2), however MinnGold produced a significantly lower amount of total dry biomass than Eiko (-26.0%; p-value=0.03; Table 2). Root and aboveground biomass was respectively 36.8% (p-value=0.03) and 24.6% (p-value=0.03) lower in MinnGold than in Eiko.

Discussion

A direct dependence of photosynthesis on plant Chl-content is often assumed, especially when remote sensing-based methods are used to estimate photosynthesis (Peng *et al*., 2011; Croft *et al*., 2017). Recent investigations on Chl-deficient mutants have instead shown that such an assumption is too simplistic, and a more careful examination of a series of mechanisms at both leaf and canopy scales is required. The observation of comparable leaf-scale photosynthetic rates in Chl-deficient and wildtypes has been reported in other studies (Li *et al*., 2013; Daloso *et al*., 2014; Kirst *et al*., 2017). In particular, Slattery *et al*., (2017) observed similar results referring to another soybean mutant (Y11y11). The small differences in the absorbance of PPFD at the Chl-absorption peak wavelengths between the Chl-deficient and green leaves can partially explain those observations (Figure 2). In green leaves, incoming blue and red light wavelengths are mostly absorbed in the adaxial layers of the leaf (Cui *et al*., 1991; Nishio, 2000), so that mostly green photons reach the chloroplasts located in the abaxial section of the leaves (Terashima *et al*., 2009). Reduced Chl concentrations facilitate a more uniform distribution of readably absorbable light across the path-length of the leaf (Slattery *et al*., 2016; Kirst *et al*., 2017). The available light energy is higher in the abaxial section of the leaves of the Chl-deficient mutant, and the greatest differences concern blue and then red wavelengths (Slattery *et al*., 2016). However, in green leaves, green photons are predominantly absorbed by the chloroplasts located in the abaxial section of the leaves, while a larger fraction of green/yellow light is transmitted and not absorbed in the Chl-deficient mutant (Figure 2; Figure S2).

The light and CO_2 response curves measured using gas exchange systems equipped with blue/red LED light source were nearly identical between Chl-deficient and green leaves of both pot- and

field-grown plants (Figure 1; Figure S1). This translated into a higher NUE_l of MinnGold as predicted by the model proposed by Song *et al*. (2017). When the light source was modified by adding green/yellow light and removing the red component (Figure S4), the quantum yield - ϕ (*i.e*. the initial slope of the A/PPFD curves), remained unchanged in green leaves (p=0.55; Figure S5). The high density of chloroplasts favored the absorption of green/yellow light (Terashima *et al*., 2011), thus leading to a compensatory effect and similar photosynthetic capacity in green leaves with both light sources. This was not the case for the leaves of the mutant, where the lack of red photons caused a 17% decrease in ϕ when compared to MN0095 (p=0.008; Table S5), because only a small fraction of the green/yellow light was absorbed by the sparser chloroplasts (Figure 2). It is well established that the light harvesting complex in leaves can be damaged by excessive light. Plants have evolved NPQ mechanisms to increase their efficiency in heat dissipation relative to the dark-adapted state (Maxwell & Johnson, 2000). NPQ variations are related to de-epoxidation and epoxidation of the xanthophyll cycle pigments, a dynamic mechanism that undergoes excitation and relaxation phases as a function of light exposure (Müller *et al*., 2001). Consistent with the recent work (Li *et al*., 2013; Gu *et al*., 2017a), when measured by means of PAM fluorescence, NPQ was reduced in the mutant and accordingly the photoprotection was lower than in the green leaves. On the other hand, reduced photoprotection led to an increase in Φ_{PSII} (Figure 3), which indicates a substantial change in the balance between photochemical and non-photochemical pathways fueling carbon fixation and mitigating photo-damage. Comparable R_{PR} in the two soybean varieties further confirmed that such an increase in Φ_{PSII} in the mutant is not due to higher carboxylation/oxygenation rates of RuBisCO (Figure 1; Table S2).

The hypothesis that similar leaf-scale photosynthetic rates, such as those observed in this study in

the Chl-deficient and green varieties, could actually translate into similar photosynthetic rates of entire canopies required further investigation. Canopy gross and net photosynthesis are in fact the result of the integration of a series of mechanisms operating at different scales. In Chl-deficient crops, different light reflectance and transmittance can be observed, but while the difference in reflectance influences the amount of radiation that reaches the plant organs, including the chloroplasts, the difference in light transmission modifies light distribution inside the canopy. The energy balance and the $APPFD_{CANOPY}$ measurements made in the large field plots enabled estimation of light reflectance and absorption of the two canopies. While the difference in albedo was large (Figure S3), the difference in light absorption ($APPFD_{CANOPY}$) was comparatively small (6.66%). Although this aspect was not investigated in detail, such a reduction was likely due to the deeper penetration and more even distribution of light within the canopy of the mutant (Drewry *et al*., 2014; Gu *et al*., 2017a). The increased photochemical efficiency of individual leaves of the mutant (Figure 3) would suggest that for a given amount of $APPFD_{CANOPY}$, GPP should have been higher in MinnGold than in Eiko. However, this was not the case (Figure 7), suggesting that the higher photochemical efficiency was enough to only offset the lower light absorption (Walker *et al*., 2017).

Concerning the nitrogen demands, our results are in line with the simulations of Walker *et al*. (2017) who demonstrated that similar rates of canopy photosynthesis can be maintained with 9% savings in leaf nitrogen resulting from decreased Chl. In our study, higher nitrogen savings were observed, as MinnGold had 24% less N per unit leaf area than Eiko (Table 1).

The observation of similar photosynthetic rates in leaves (Figure 1 and Figure S1) and canopies (Figure 7) of the Chl-deficient mutant and the green accessions was not consistent with the

observation that total dry mass at the end of field experiment was significantly lower in MinnGold than in Eiko (-26.0%; Table 2). If photosynthetic rates were almost identical, the overall amount of carbon accumulated by the plants should have also been the same. The differences in plant biomass could therefore be the result of other processes, which are not entirely accounted for by steady state photosynthesis measurements. In this regard, some studies highlighted the relative importance of dynamic photosynthesis to the overall C-uptake of plants and crops (Zhu *et al*., 2004). Kromdijk *et al*. (2016) showed that the NPQ relaxation that occurs after a drop in incoming radiation can substantially affect carbon uptake. The rate of recovery from the quenched to the unquenched state is related to the decrease in the quantum efficiency of plants, after the transition from high to low light intensity, which may potentially account for up to a 30% reduction of carbon fixation (Zhu *et al*., 2004). In our study, the comparison of NPQ relaxation dynamics highlighted a significant difference between MinnGold and Eiko, as the NPQ of the mutant decreased slower (Figure 4). The consequence of different relaxation dynamics was a change in dynamic photosynthesis: in the leaves of Eiko, the recovery towards the steady state photosynthetic rates was much faster than in MinnGold. This illustrates how NPQ relaxation might have contributed to dynamic photosynthesis of the two accessions and with this to their overall net carbon fixation during the crop cycle. Following Kromdijk *et al*. (2016) we may in fact state that "*light conditions in the field are anything but steady state"*. Decelerated NPQ relaxation observed in the mutant might substantially diminish the quantum efficiency of photosynthesis during light transition events (*i.e*. clouds and/or self-shading sun flecks), thus leading to an overall lower productivity even if the steady state photosynthetic capacity is the same for both accessions.

In conclusion, our study reveals that the steady state photosynthesis of a Chl-deficient soybean

mutant is comparable to that of green varieties, and this result applies to both the leaf and the canopy scales. Carbon-uptake rates of crops are not a simple function of their chlorophyll content, as better light distribution in the canopy and increased photochemical efficiency may compensate for reduced light absorption of individual leaves, when chlorophyll content is significantly reduced. However, Chl-deficiency may affect NPQ relaxation dynamics, which may be responsible for reduced net carbon assimilation over time, considering that rapid and frequent light fluctuations naturally occur in the field.

New accessions can be potentially developed, where the genes regulating synthesis of xanthophylls may be overexpressed to compensate for such a decrease in dynamic photosynthesis (Kromdijk *et al*., 2016). When successful, this strategy could lead to the creation of a new generation of crop plants, which may achieve similar yields to traditional cultivars, while reflecting more shortwave radiation via an increase in albedo. There is an increasing consensus that modification of crop albedo is likely to be one of the most effective solar radiation management strategies, capable of mitigating a significant fraction of current global warming (Hirsch *et al*., 2017; Ridgwell *et al*., 2009; Davin *et al*., 2014; Bright *et al*., 2016) and, as demonstrated in this paper, serve as a pathway towards reduced water use in agriculture.

Aknowledgements

The authors have no conflict of interest to declare. The authors thank Alessandro Boz, Melissa Morabito, Nike Basso, Marin Tudoroiu, Stefano Nannarelli, Alberto Mattedi, Silvia Baronti, Marcin Stróżecki and Diego Chiabà for the help during field sampling and lab analysis. During data acquisition, K.S. was supported by a Ph.D. grant from Fondazione Edmund Mach, San

Michele all'Adige, Italy and the COST Action ES1309/OPTIMISE. G.A. was partially supported during paper preparation by a scholarship from the German Academic Exchange Service (DAAD, Germany) for a three-month research period at University of Freiburg, Germany. The funders had no role in study design, data collection and analysis, decision to publish, or preparation of the manuscript. In 2017, the data were acquired within an airborne FLuorescence EXplorer (FLEX) campaign supported by the European Space Agency (Contract No. 4000107143/12/NL/FF/If). This work contributes to Photosynthesis 2.0 MIUR-FOE-2015.

Author contributions

K.S., L.G., G.A., A.P., G.D.V., D.G., M.Ros., B.W.C., U.R. and F.M. designed the study; K.S., L.G., G.A., A.P., G.D.V., C.P., M.C., L.V., R.J., M.Rod., J-P.M., R.C., M.P.C-M. did the measurements in the field; K.S., L.G., G.A., A.P., G.D.V., C.P., M.H., M.Rod., R.J. and F.M. performed the analyses; K.S., G.A., L.G., A.P., M.H. and F.M. wrote the first version of the manuscript, which was intensively discussed and revised by all authors.

References

Acosta M., Juszczak R., Chojnicki B., Pavelka M., Havrànková K., Lesny J., … Olejnik J. (2017) CO_2 fluxes from different vegetation communities on a peatland ecosystem. *Wetlands* **37**, 423–435.

Benedict C.R., McCree K.J. & Kohel R.J. (1972) High Photosynthetic Rate of a Chlorophyll Mutant of Cotton. *Plant physiology* **49**, 968–971.

Bright R.M., Bogren W., Bernier P. & Astrup R. (2016) Carbon-equivalent metrics for albedo changes in land management contexts: relevance of the time dimension. *Ecological Applications* **26**, 1868–1880.

Campbell B.W., Mani D., Curtin S.J., Slattery R.A., Michno J.-M., Ort D.R., … Stupar R.M. (2014) Identical substitutions in magnesium chelatase paralogs result in chlorophyll-deficient soybean mutants. *G3 (Bethesda, Md.)* **5**, 123–31.

Croft H., Chen J.M., Luo X., Bartlett P., Chen B. & Staebler R.M. (2017) Leaf chlorophyll content as a proxy for leaf photosynthetic capacity. *Global Change Biology* **23**, 3513–3524.

Cui M., Vogelmann T.C. & Smith W.K. (1991) Chlorophyll and light gradients in sun and shade leaves of Spinacia oleracea. *Plant, Cell and Environment* **14**, 493–500.

Daloso D. de M., Antunes W.C., Santana T.A., Pinheiro D.P., Ribas R.F., Sachetto-Martins G. & Loureiro M.E. (2014) Arabidopsis gun4 mutant have greater light energy transfer efficiency in photosystem II despite low chlorophyll content. *Theoretical and Experimental Plant Physiology* **26**, 177–187.

Davin E.L., Seneviratne S.I., Ciais P., Olioso A. & Wang T. (2014) Preferential cooling of hot extremes from cropland albedo management. *Proceedings of the National Academy of*

Sciences **111**, 9757–9761.

Drewry D.T., Kumar P. & Long S.P. (2014) Simultaneous improvement in productivity, water use, and albedo through crop structural modification. *Global Change Biology* **20**, 1955–1967.

Ethier G.J. & Livingston N.J. (2004) On the need to incorporate sensitivity to CO_2 transfer conductance into the Farquhar–von Caemmerer–Berry leaf photosynthesis model. *Plant, Cell and Environment* **27**, 137–153.

Gengenbach B.G., Gorz H.J. & Haskins F. (1970) Genetic Studies of Induced Mutants in Melilotus alba. II. Inheritance and Complementation of Chlorophyll-deficient Mutants. *Crop Science* **10**, 154–156.

Gu J., Zhou Z., Li Z., Chen Y.,Wang Z. & Zhang, H. (2017a) Rice (*Oryza sativa* L.) with reduced chlorophyll content exhibit higher photosynthetic rate and efficiency, improved canopy light distribution, and greater yields than normally pigmented plants. *Field Crop Res*. **200**, 58–70.

Gu J., Zhou Z., Li Z., Chen Y., Wang Z., Zhang H. & Yang J. (2017b) Photosynthetic Properties and Potentials for Improvement of Photosynthesis in Pale Green Leaf Rice under High Light Conditions. *Frontiers in Plant Science* **8**:1082.

Highkin H. (1950) Chlorophyll studies on barley mutants. *Plant Physiology* **25**, 294–306.

Hirsch A.L., Wilhelm M., Davin E.L., Thiery W. & Seneviratne S.I. (2017) Can climate-effective land management reduce regional warming? *Journal of Geophysical Research: Atmospheres* **122**, 2269–2288.

Hoffmann M., Jurisch N., Albiac Borraz E., Hagemann U., Drösler M., Sommer M. & Augustin

J. (2015) Automated modeling of ecosystem CO_2 fluxes based on periodic closed chamber measurements: A standardized conceptual and practical approach. *Agricultural and Forest Meteorology* **200**, 30–45.

Juszczak R., Acosta M. & Olejnik J. (2012) Comparison of daytime and nighttime ecosystem respiration measured by the closed chamber technique on a temperate mire in Poland. *Polish J. Environ. Stud.* **21**, 643–658.

Keys A., Sampaio E., Cornelius M. & Bird I. (1977) Effect of Temperature on Photosynthesis and Photorespiration of Wheat Leaves. *Journal of Experimental Botany* **28**, 525–533.

Kirst, H., Gabilly, S.T., Niyogi, K.K., Lemaux, P.G. & Melis, A. (2017) Photosynthetic antenna engineering to improve crop yields. Planta **245**, 1009-1020.

Kromdijk J., Głowacka K., Leonelli L., Gabilly S.T., Iwai M., Niyogi K.K. & Long S.P. (2016) Improving photosynthesis and crop productivity by accelerating recovery from photoprotection. *Science* **354**, 857–861.

Li Y., Ren B., Gao L., Ding L., Jiang D., Xu X., … Guo S. (2013) Less Chlorophyll Does not Necessarily Restrain Light Capture Ability and Photosynthesis in a Chlorophyll-Deficient Rice Mutant. *Journal of Agronomy and Crop Science* **199**, 49–56.

Lichtenthaler H.K. (1987) Chlorophylls and carotenoids: Pigments of photosynthetic biomembranes. *Methods in Enzymology* **148**, 350–382.

Long S.P., Zhu X.-G., Naidu S.L. & Ort D.R. (2006) Can improvement in photosynthesis increase crop yields? *Plant, Cell and Environment* **29**, 315–330.Müller P., Li X.P. & Niyogi K.K. (2001) Non-photochemical quenching. A response to excess light energy. *Plant physiology* **125**, 1558–66.

Nishio J.N. (2000) Why are higher plants green? Evolution of the higher plant photosynthetic pigment complement. *Plant, Cell and Environment* **23**, 539–548.

Ort D.R. & Melis A. (2011) Optimizing antenna size to maximize photosynthetic efficiency. *Plant physiology* **155**, 79–85.

Peressotti A. & Ham J.M. (1996) A Dual-Heater Gauge for Measuring Sap Flow with an Improved Heat-Balance Method. **155**, 149–155.

Ridgwell A., Singarayer J.S., Hetherington A.M. & Valdes P.J. (2009) Tackling regional climate change by leaf albedo bio-geoengineering. *Current Biology* **19**, 146–50.

Sakuratani T. (1981) A Heat Balance Method for Measuring Water Flux in the Stem of Intact Plants. *Journal of Agricultural Meteorology* **37**, 9–17.

Slattery R.A., Grennan A.K., Sivaguru M., Sozzani R. & Ort D.R. (2016) Light sheet microscopy reveals more gradual light attenuation in light-green versus dark-green soybean leaves. *Journal of Experimental Botany* **67**, 4697-4709.

Slattery R.A., VanLoocke A., Bernacchi C.J., Zhu X.-G. & Ort D.R. (2017) Photosynthesis, Light Use Efficiency, and Yield of Reduced-Chlorophyll Soybean Mutants in Field Conditions. *Frontiers in Plant Science* **8**, 549.

Song Q., Wang Y., Qu M., Ort D.R. & Zhu X.-G. (2017) The impact of modifying photosystem antenna size on canopy photosynthetic efficiency—Development of a new canopy photosynthesis model scaling from metabolism to canopy level processes. *Plant, Cell and Environment* **40**, 2946–2957.

Specht J., Haskins F. & Gorz H. (1975) Contents of chlorophylls a and b in chlorophyll-deficient mutants of sweetclover. *Crop Science* **15**, 851–853.

Terashima I., Fujita T., Inoue T., Chow W.S. & Oguchi R. (2009) Green light drives leaf photosynthesis more efficiently than red light in strong white light: revisiting the enigmatic question of why leaves are green. *Plant & cell physiology* **50**, 684–97.

Terashima I., Hanba Y.T., Tholen D. & Niinemets Ü. (2011) Leaf functional anatomy in relation to photosynthesis. *Plant physiology* **155**, 108–16.

Walker B.J., Drewry D.T., Slattery R.A., VanLoocke A., Cho Y.B. & Ort D.R. (2017) Chlorophyll can be reduced in crop canopies with little penalty to photosynthesis. *Plant Physiology* **176**, 1215-1232.

Vogelmann T.C., Bornman J.F. & Yates D.J. (1996) Focusing of light by leaf epidermal cells. *Physiologia Plantarum* **98**, 43–56.

Vogelmann T.C. & Evans J.R. (2002) Profiles of light absorption and chlorophyll within spinach leaves from chlorophyll fluorescence. *Plant, Cell and Environment* **25**, 1313–1323.

Van Wittenberghe S., Alonso L., Verrelst J., Hermans I., Delegido J., Veroustraete F., … Samson R. (2013) Upward and downward solar-induced chlorophyll fluorescence yield indices of four tree species as indicators of traffic pollution in Valencia. *Environmental Pollution* **173**, 29–37.

Zamft B.M. & Conrado R.J. (2015) Engineering plants to reflect light: strategies for engineering water-efficient plants to adapt to a changing climate. *Plant Biotechnology Journal* **13**, 867–74.

Zhu X.-G., Ort D.R., Whitmarsh J. & Long S.P. (2004) The slow reversibility of photosystem II thermal energy dissipation on transfer from high to low light may cause large losses in carbon gain by crop canopies: a theoretical analysis. *Journal of Experimental Botany* **55**, 1167–1175.

Tables

Table 1. Summary of leaf properties of plants grown in the field in the growing season of 2015 and 2016. Chlorophyll content, specific leaf mass and nitrogen content are reported with the ratio of Ch-deficient MinnGold as compared with green MN0095 and Eiko, in 2015 and 2016, respectively. Values represent mean ± standard error. The Mann-Whitney-Wilcoxon test was used to compare the two accessions.

	MN0095 (2015)	**MinnGold (2015)**	**Ratio MinnGold: MN0095**	**Eiko (2016)**	**MinnGold (2016)**	**Ratio MinnGold: Eiko**
Total chlorophyll content (μg cm^{-2})	39.66±1.31 (n=15)	8.65±0.62 (n=15)	0.22 (p<0.001)	50.03±2.57 (n=12)	11.03±0.62 (n=16)	0.22 (p<0.001)
Specific leaf mass (g m^{-2})	50.94±0.95 (n=15)	34.48±1.41 (n=15)	0.68 (p<0.001)	44.98±1.22 (n=4)	31.38±0.35 (n=4)	0.70 (p=0.0286)
Nitrogen content (gN g^{-1})	0.054±0.001 (n=15)	0.063±0.001 (n=15)	1.17 (p<0.001)	0.052±0.001 (n=4)	0.056±0.002 (n=4)	1.08 (p=0.0571)
Nitrogen content (gN m^{-2})	2.75±0.07 (n=15)	2.17±0.11 (n=15)	0.79 (p<0.001)	2.33±0.05 (n=4)	1.76±0.05 (n=4)	0.76 (p=0.0286)

Table 2. Plant density, leaf area index (LAI), above- and belowground dry biomass and total dry biomass of the field-grown green (Eiko) and Chl-deficient (MinnGold) varieties measured at the end of canopy flux measurements (July 27th, 2016). Values represent mean ± standard error (n=4). The Mann-Whitney-Wilcoxon test was used to compare the two accessions.

	Eiko	**MinnGold**	**% Difference**	**p-value**
Plant density (n m^{-2})	34±1	36±1	6.6%	0.20
LAI (m^2 m^{-2})	10.1±0.6	10.1±0.2	-0.2%	1
Aboveground biomass (g m^{-2})	857±53	647±16	-24.6%	0.03
Belowground biomass (g m^{-2})	118±7	74±2	-36.8%	0.03
Total biomass (g m^{-2})	975±60	721±17	-26.0%	0.03

Figures

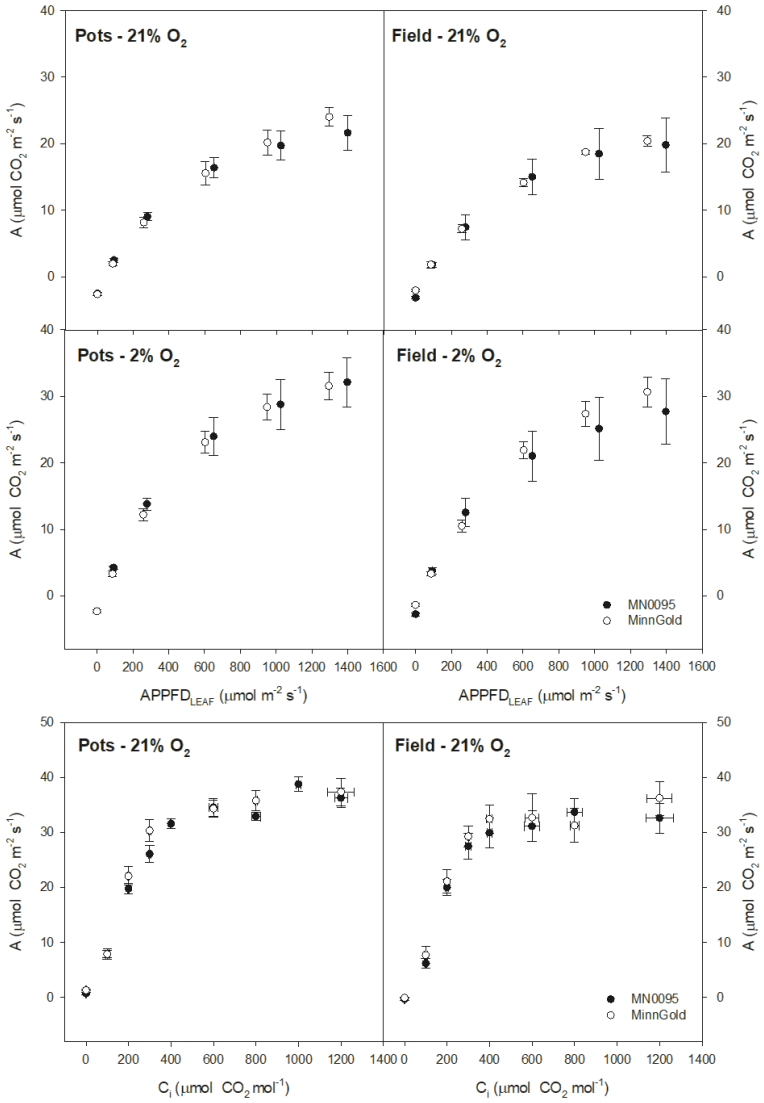

Figure 1. A/APPFD$_{LEAF}$ response curves measured under ambient and 2% O_2 concentration and A/C_i response curves measured under ambient O_2 on green (MN0095, filled circles) and Chl-deficient (MinnGold, open circles) leaves of pot- (n=5 for both A/APPFD$_{LEAF}$ and A/C_i response curves) and field-grown (n=3 for A/APPFD$_{LEAF}$ and n=6 for A/C_i response curves) plants. Each symbol represents mean ± standard error.

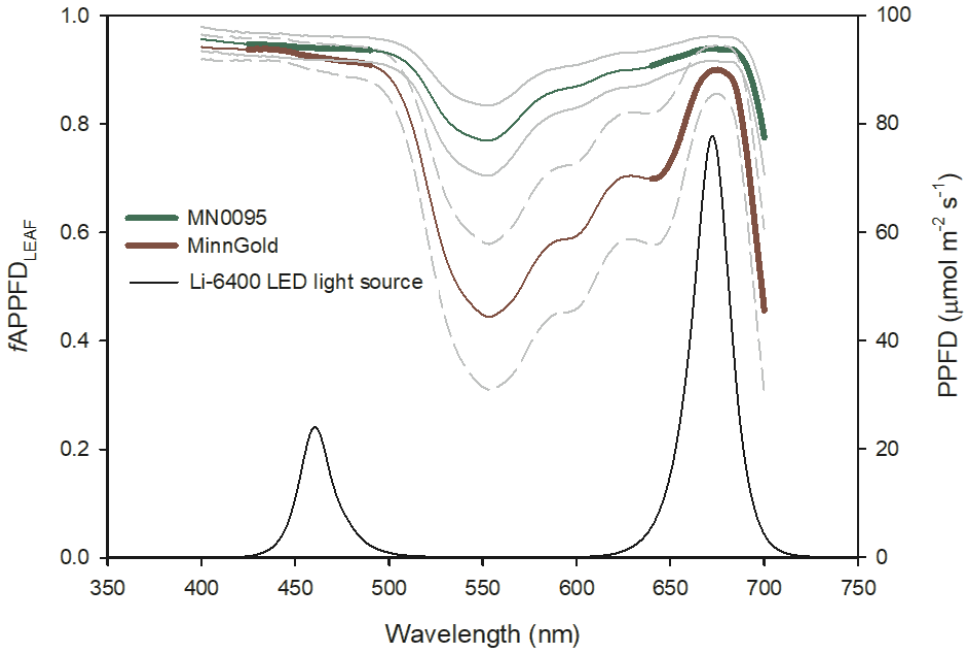

Figure 2. Fraction of photosynthetic photon flux density absorbed by the most recently fully-developed leaves (fAPPFD$_{LEAF;}$ -) (n=16) measured in 2015 on field-grown plants under natural irradiance. The thick solid lines (MN0095=green and MinnGold=red) indicate the light regions where photosynthesis was measured (425-490 and 640-700 nm) using the Li-6400 LED light source. The grey solid and dashed lines represent the 95% confidence interval. The light spectrum and intensity of the LED light source is also shown.

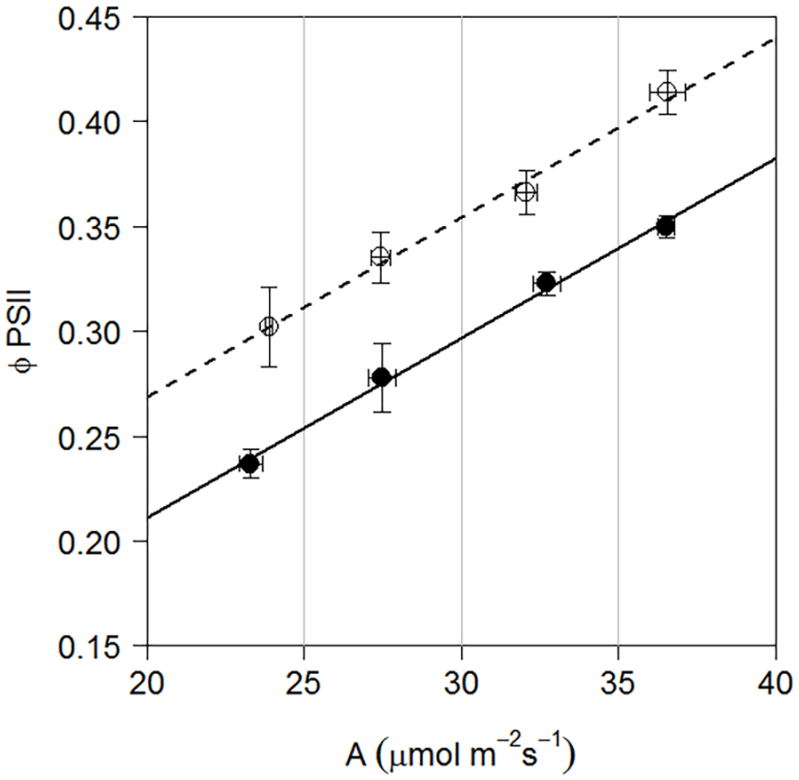

Figure 3. Relationship between Photosystem II efficiency - Φ_{PSII} and net assimilation rate of CO_2 - A for green (MN0095, black circles, solid trend line) and Chl-deficient (MinnGold, open circles, dashed trend line) leaves. Each symbol represents mean ± standard error of measurements averaged over classes indicated by the grey solid vertical lines. The total number of replicates for MN0095 and MinnGold in the 20-40 μmol m^{-2} s^{-1} assimilation range was equal to 38 and 35, respectively.

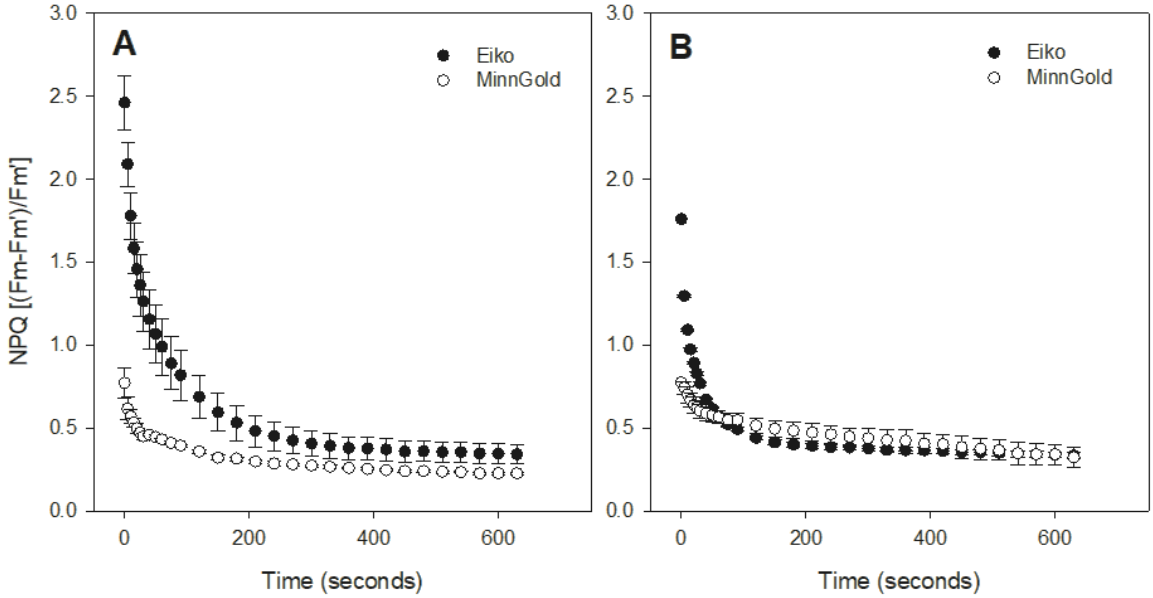

Figure 4. Non-photochemical quenching (NPQ) relaxation in unifoliate (panel A) and trifoliate (panel B) leaves measured on pot-grown plants in the laboratory conditions. Each symbol represents mean ± standard error (n=4). Closed and open symbols indicate Eiko and MinnGold leaves, respectively.

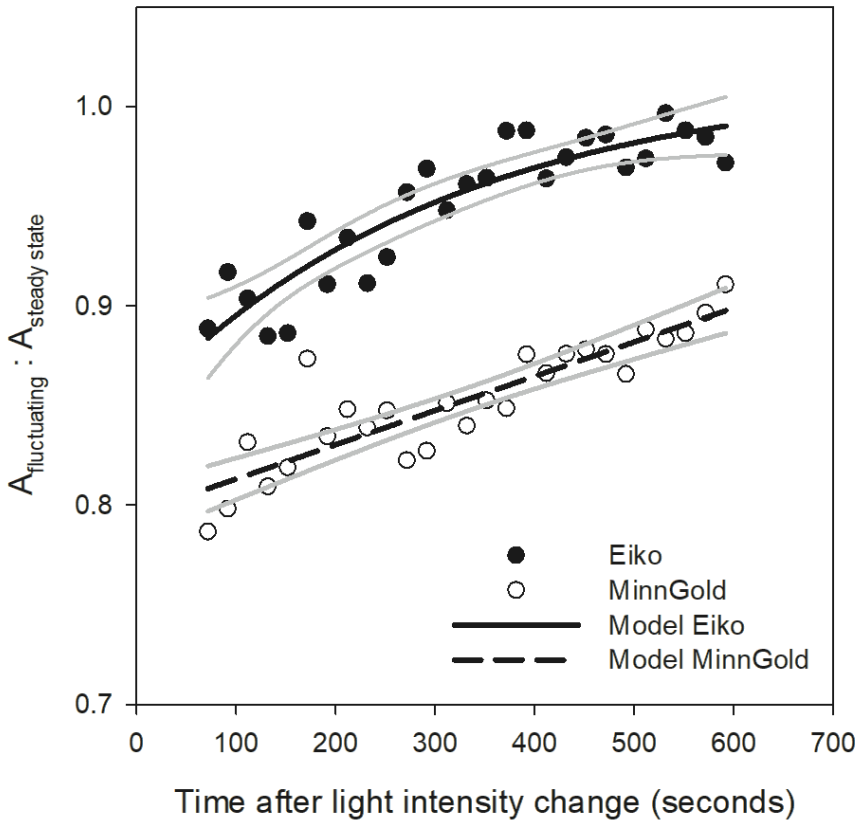

Figure 5. Time course of net CO_2 fixation rate ($A_{fluctuating}$), normalized by the steady state net CO_2 fixation rate ($A_{steady\ state}$) at 200 μmol photons m^{-2} s^{-1}, during zeaxanthin-dependent quenching (qZ). Closed and open symbols indicate Eiko and MinnGold leaves, respectively; solid and dashed lines indicate regression models for Eiko ($Y=0.85+0.16*(1-exp^{-0.003*X})$; $R^2=0.82$; $p<0.0001$) and MinnGold ($Y=0.0002*X+0.80$; $R^2=0.78$; $p<0.0001$), respectively; grey lines indicate 95% confidence intervals. Each symbol represents the mean of 4 measurements.

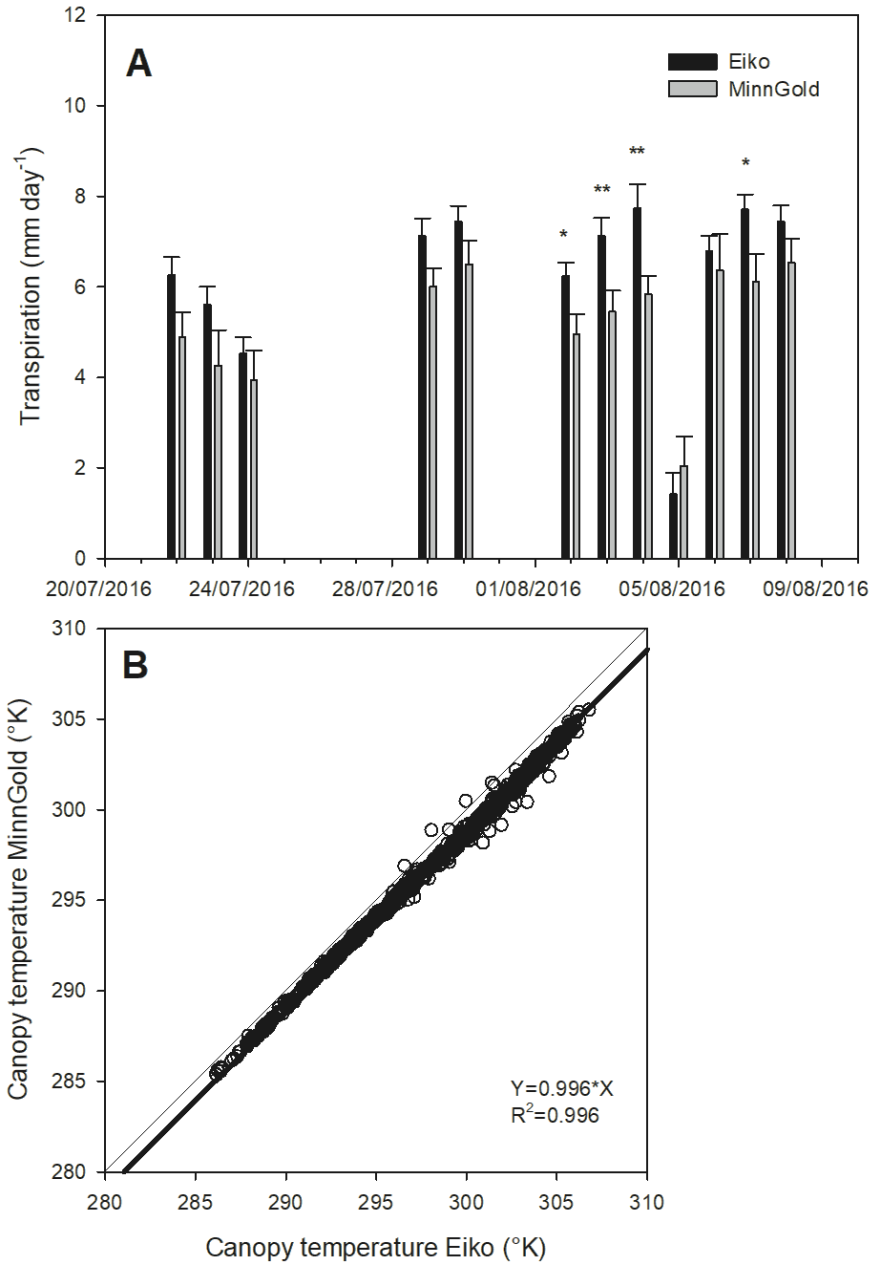

Figure 6. Panel A: Daily plant transpiration (mm day^{-1}) measured in 2016 in the field with sap flow gauges (mean ± standard error; n=10). Panel B: regression between MinnGold and Eiko canopy temperature. The thin line represents the 1:1 line. Two-way ANOVA: * p-value<0.05; ** p-value<0.01; *** p-value<0.001.

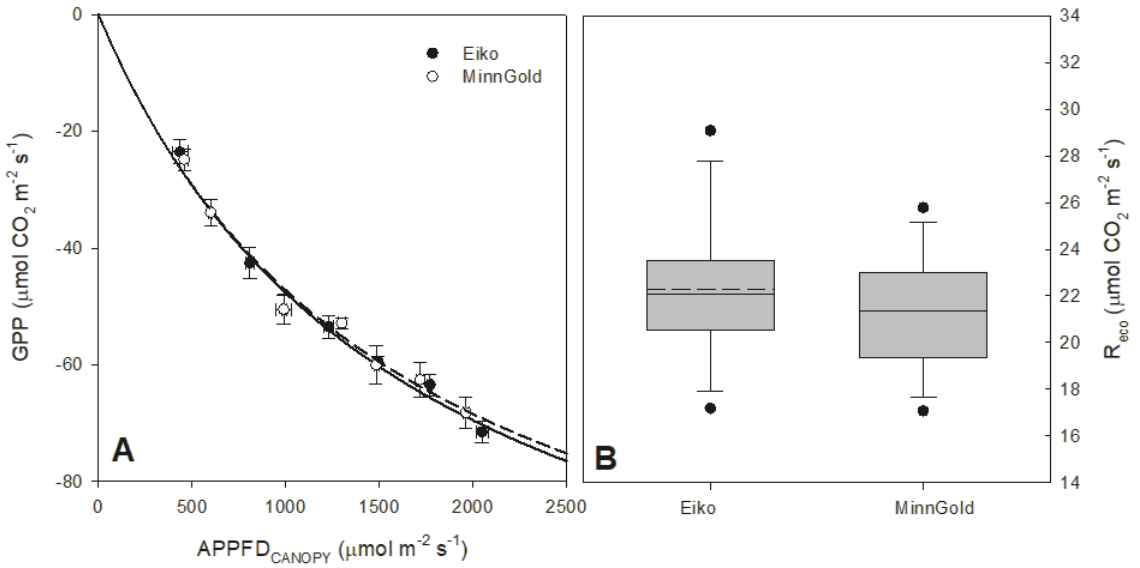

Figure 7. Gross primary production (GPP) vs. photosynthetic photon flux density absorbed by the canopy ($APPFD_{CANOPY}$) (panel A) and ecosystem respiration (R_{eco}) (panel B) measured in the field in 2016. $APPFD_{CANOPY}$ was estimated by multiplying the incident PPFD by the fraction of PPFD absorbed by the vegetation canopy ($fAPPFD_{CANOPY}$). In panel A, solid and dashed lines represent the regression lines for green (Eiko) and Chl-deficient (MinnGold) canopies, respectively; vertical and horizontal bars represent standard error (n=4).